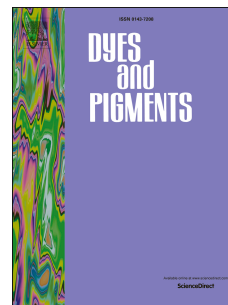


# Accepted Manuscript

Photophysical and electrochemical studies of highly fluorescent pyrazole and imidazole containing heterocycles

Hardesh K. Maurya, Ch. Pavan Kumar, M. Chandrasekharam, Atul Gupta



PII: S0143-7208(16)30720-3

DOI: [10.1016/j.dyepig.2016.09.030](https://doi.org/10.1016/j.dyepig.2016.09.030)

Reference: DYPI 5482

To appear in: *Dyes and Pigments*

Received Date: 15 June 2016

Revised Date: 5 September 2016

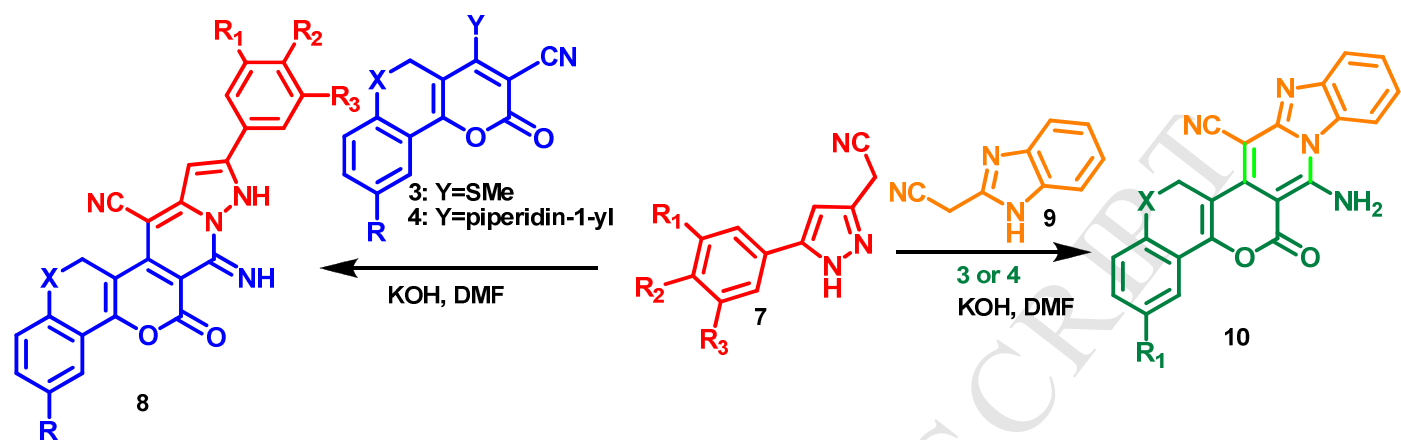
Accepted Date: 12 September 2016

Please cite this article as: Maurya HK, Kumar CP, Chandrasekharam M, Gupta A, Photophysical and electrochemical studies of highly fluorescent pyrazole and imidazole containing heterocycles, *Dyes and Pigments* (2016), doi: 10.1016/j.dyepig.2016.09.030.

This is a PDF file of an unedited manuscript that has been accepted for publication. As a service to our customers we are providing this early version of the manuscript. The manuscript will undergo copyediting, typesetting, and review of the resulting proof before it is published in its final form. Please note that during the production process errors may be discovered which could affect the content, and all legal disclaimers that apply to the journal pertain.

## Photophysical and electrochemical studies of highly fluorescent pyrazole and imidazole containing heterocycles

Hardesh K. Maurya, CH. Pavan Kumar, M. Chandrasekharam,\* Atul Gupta\*



# Photophysical and electrochemical studies of highly fluorescent pyrazole and imidazole containing heterocycles

Hardesh K. Maurya<sup>a</sup>, Ch. Pavan Kumar<sup>b,c</sup>, M. Chandrasekharam<sup>\*b,c</sup>, Atul Gupta<sup>\*#a</sup>

<sup>a</sup> Medicinal Chemistry Department, Central Institute of Medicinal and aromatic Plants, PO. CIMAP, Kukrail Road, Lucknow-226015, India

<sup>b</sup> CSIR-Indian Institute of Chemical Technology, I&PC Division, Uppal Road, Tarnaka, Hyderabad - 500 607, India.

<sup>c</sup> Academy of Scientific and Innovative Research, CSIR-IICT, Hyderabad - 500 607, India

*Keywords:* pyran-2-one, benzo[*h*]chromene, thiochromeno[4,3-*b*]pyran, fluorescence, TDDFT

**Corresponding Author**

**\*Atul Gupta, Tel.: 0915222718556, E-mail: atisky2001@yahoo.co.in (A. G.),**

**Abstract**

Highly congested pyrazole and imidazole ring containing heterocycles were studied for their photophysical and electrochemical properties. TDDFT calculations of the molecules were carried out using B3LYP/G(d,p) level theory in DMF medium and the results were in good agreement with the experimental values. The imidazole derivatives showed a red shifted absorption peak ( $\lambda_{\text{max}}$ , 455-474 nm) and higher molar extinction coefficient than pyrazole derivatives. In the case of increasing  $\pi$ -conjugation from pyrazoles to imidazoles red shift in the emission maxima (537 nm-565 nm) was observed. These preliminary results of absorption and emission spectroscopy illustrate that these molecules may have potential organic electronic applications.

## 1 INTRODUCTION

Fluorescent organic compounds are of immense interest in many areas such as functional materials in organic light-emitting devices (OLEDs) [1–3], photovoltaics [4,5], structure, dynamics, dyes for polymers and textile [6], These molecules can also be used as functions of biomolecules studies [7,8], labels and probes for coloring of malignancies in image-guided surgery [9,10]. The multifarious uses of fluorophores arouse the demand and interest for the synthesis of newer fluorescent compounds with desired properties.

Based on their applicability in the natural light harvesting systems, porphyrins have been extensively explored as effective photofluorescent agents. It was realized that for photophysical activity of these molecules, structural planarity and dominant  $\pi$ -electron density (highly conjugated system) is essentially required. Based on these observations, various other photofluorescent organic compounds incorporating coumarin, indoline, phenothiazine, fluorene, carbazole, pyrazole, imidazole, triphenylamine and tetrahydroquinoline nucleus have been studied as bio-imaging agents [11], fluorescent probes [12], chemosensors [13], electroluminescent materials for organic electronics [14] light harvesting agents [15], transistor devices [16], photovoltaic cells [17] and OLEDs [18]. Development of Sulforhodamine B [19] (**i**, a bioimaging dye), bodipy [20] (**ii**, visible fluorescence chemosensor), PTPOBS [21] (**iii**, hole-transporters in OLEDs) and tris(8-hydroxyquinolino)aluminum (**iv**) [22] (blue luminescent in OLEDs) are some notable examples in this regards Fig. 1.

As a part of on going program to design and develop fluorescent sensitizers, we have studied photophysical and electrochemical properties of highly congested pyrazole and imidazole based heterocycles. Most of the compounds possess rod like configuration with high  $\pi$ -electron charge density in conjugation with nitrogen atoms usually present in the organic dyes.

<<Insert Figure-1>>

## 2. Experimental details

The reagents and solvents used in this study were of analytical or laboratory grade and used without further purification unless stated otherwise. All the reactions were monitored on Merck aluminium silica gel thin layer chromatography (TLC, UV<sub>254nm</sub>) plates. Column chromatography was carried out on silica gel (100-200 mesh). The melting points were determined on Buchi melting point M560 apparatus in open capillaries and are uncorrected. <sup>1</sup>H (300 MHz) and <sup>13</sup>C NMR (75 MHz) spectra were recorded on a Bruker WM-300 using CDCl<sub>3</sub> as reference solvent. Chemical shifts ( $\delta$ -value) are reported in parts per million (ppm) Signal patterns are indicated as s, singlet; bs, broad singlet; d, doublet; dd, double doublet; t, triplet; m, multiplet. Coupling constants (*J*) are given in Hertz. Infrared (IR) spectra were recorded on a Perkin-Elmer AX-1 spectrophotometer in KBr disc and reported in wave number (cm<sup>-1</sup>). ESI-MS mass spectra were recorded on Shimadzu LC-MS and/or LC-MS-MS APC3000 (Applied Biosystem). IUPAC nomenclature was recorded on Chem Draw-15.

2.1. *General procedure for the synthesis of 7-imino-6-oxo-10-aryl-7,9,13,14-tetrahydro-6H-benzo[7,8]chromeno[4,3-d]pyrazolo[1,5-a]pyridine-12-carbonitriles (8a-c)/ 7-imino-6-oxo-10-aryl-7,9-dihydro-6H,13H-pyrazolo[1,5-a]thiochromeno[3',4':5,6]pyrano[4,3-d]pyridine-12-carbonitrile (8d-h)* [23]

A mixture of lactone **3** (1.0 mmol), 2-(5-aryl-1H-pyrazol-3-yl)acetonitrile (**7**, 1.0 mmol) and powdered KOH (1.2 mmol) in DMF (9 mL) was stirred at room temperature for 5-8 h. The reaction was monitored using silica gel TLC. After consumption of **3**, the crude residue was poured onto crushed ice with vigorous stirring. The aqueous suspension was neutralized with dil. HCl (if required) and the precipitate obtained was filtered, washed with water and dried. Residue was purified by silica gel column chromatography using chloroform/methanol (0-30%);

**7-Imino-6-oxo-10-phenyl-7,9,13,14-tetrahydro-6H-benzo[7,8]chromeno[4,3-d]pyrazolo[1,5-a]pyridine-12-carbonitrile (8a)**

Yellow solid; yield 67%; mp: 303-304°C;  $R_f$  0.38 ( $\text{CHCl}_3$ ); IR (KBr): 1577, 1611, 1692 (C=O), 2203 (CN), 3259 and 3370 (NH)  $\text{cm}^{-1}$ ;  $^1\text{H}$  NMR (300 MHz, DMSO- $d_6$ ):  $\delta$  2.94 (t, 2H,  $J=7.2$  Hz,  $\text{CH}_2$ ), 3.21 (t, 2H,  $J=7.8$  Hz,  $\text{CH}_2$ ), 6.61 (s, 1H, CH), 7.28-7.48 (m, 7H, Ar-H & NH), 7.64 (m, 1H, Ar-H), 8.02 (d, 3H,  $J=7.5$  Hz, Ar-H); MS: 403.1 (M-H) $^+$ ; Anal. Calcd ( $\text{C}_{25}\text{H}_{16}\text{N}_4\text{O}_2$ ): C, 74.25; H, 3.99; N, 13.85 Found: C, 74.12; H, 3.96; N, 13.78; HRMS (ESI): calc. for  $\text{C}_{25}\text{H}_{17}\text{N}_4\text{O}_2$ : 405.1346 ( $\text{M}^+\text{+H}$ ); found: 405.1368.

**7-Imino-6-oxo-10-(4-methoxyphenyl)-7,9,13,14-tetrahydro-6H-benzo[7,8]chromeno[4,3-d]pyrazolo[1,5-a]pyridine-12-carbonitrile (8b)**

Yellow solid; yield: 60%; mp: 280-281°C;  $R_f$  0.32 (DCM); IR (KBr): 1591, 1696 (C=O), 2206 (CN), 3292 and 3409 (NH)  $\text{cm}^{-1}$ ;  $^1\text{H}$  NMR (300 MHz, DMSO- $d_6$ ):  $\delta$  2.94 (t, 2H,  $J=7.2$  Hz,  $\text{CH}_2$ ), 3.16 (t, 2H,  $J=7.2$  Hz,  $\text{CH}_2$ ), 3.78 (s, 3H, OMe), 6.54 (s, 1H, CH), 6.95 (m, 3H, Ar-H & NH), 7.30 (m, 3H, Ar-H), 7.64 (s, 1H, Ar-H), 7.94 (d, 2H,  $J=8.1$  Hz, Ar-H), 8.27 (s, 1H, NH); MS: 433.1 (M-H) $^+$ ; Anal. Calcd ( $\text{C}_{26}\text{H}_{18}\text{N}_4\text{O}_3$ ): C, 71.88; H, 4.18; N, 12.90 Found: C, 71.76; H, 4.16; N, 12.84; HRMS (ESI): calc. for  $\text{C}_{26}\text{H}_{19}\text{N}_4\text{O}_3$ : 435.1451 ( $\text{M}^+\text{+H}$ ); found: 435.1472.

**7-Imino-3-methoxy-6-oxo-10-phenyl-7,9,13,14-tetrahydro-6H-benzo[7,8]chromeno[4,3-d]pyrazolo[1,5-a]pyridine-12-carbonitrile (8c)**

Yellow solid; yield: 79%; mp: 305-306°C;  $R_f$  0.80 ( $\text{CHCl}_3$ ); IR (KBr): 1572, 1693 (C=O), 2203 (CN), 3286 and 3429 (NH)  $\text{cm}^{-1}$ ;  $^1\text{H}$  NMR (300 MHz, DMSO- $d_6$ ):  $\delta$  2.91 (t, 2H,  $J=7.5$  Hz,  $\text{CH}_2$ ), 3.17 (t, 2H,  $J=7.5$  Hz,  $\text{CH}_2$ ), 3.79 (s, 3H, OMe), 6.58 (s, 1H, CH), 6.88 (m, 3H, Ar-H & NH), 7.42 (m, 3H, Ar-H), 7.64 (s, 1H, Ar-H), 7.55 (m, 1H, Ar-H), 8.01 (d, 1H,  $J=7.2$  Hz, Ar-H), 8.27 (s, 1H, NH); MS: 433.2 (M-

H)<sup>+</sup>; Anal. Calcd (C<sub>26</sub>H<sub>18</sub>N<sub>4</sub>O<sub>3</sub>): C, 71.88; H, 4.18; N, 12.90 Found: C, 71.80; H, 4.15; N, 12.86; HRMS (ESI): calc. for C<sub>26</sub>H<sub>19</sub>N<sub>4</sub>O<sub>3</sub>: 435.1451 (M<sup>+</sup>+H); found: 435.1475.

**7-Imino-6-oxo-10-phenyl-7,9-dihydro-6*H*,13*H*-pyrazolo[1,5-*a*]thiochromeno[3',4':5,6]pyrano[4,3-*d*]pyridine-12-carbonitrile (8d)**

Yellow solid; yield: 68%; mp: 290°C (start to decompose); R<sub>f</sub> 0.46 (CHCl<sub>3</sub>); IR (KBr): 1586, 1690 (C=O), 2208 (CN), 3305 and 3436 (NH) cm<sup>-1</sup>; <sup>1</sup>H NMR (300 MHz, DMSO-*d*<sub>6</sub>): δ 4.43 (s, 2H, SCH<sub>2</sub>), 6.65 (s, 1H, CH), 7.30-7.45 (m, 7H, Ar-H & NH), 7.74 (d, 1H, *J*=7.5 Hz, Ar-H), 8.02 (d, 3H, *J*=7.5 Hz, Ar-H); <sup>13</sup>C NMR (75 MHz, DMSO-*d*<sub>6</sub>): δ 25.05, 68.76, 88.12, 95.59, 106.96, 121.48, 126.08, 127.02, 127.28 (2C), 127.87, 128.55, 129.35, 129.43 (2C), 131.17, 133.32, 134.88, 140.56, 143.05, 150.56, 153.38, 153.75, 161.72; MS: 421.1 (M-H)<sup>+</sup>; HRMS (ESI): calc. for C<sub>25</sub>H<sub>15</sub>N<sub>4</sub>O<sub>2</sub>S: 423.0916 (M<sup>+</sup>+H); found: 423.0964.

**7-Imino-6-oxo-10-(4-methoxyphenyl)-7,9-dihydro-6*H*,13*H*-pyrazolo[1,5-*a*]thiochromeno[3',4':5,6]pyrano[4,3-*d*]pyridine-12-carbonitrile (8e)**

Yellow solid; yield: 61%; mp: 280°C (start to decompose); R<sub>f</sub> 0.14 (CHCl<sub>3</sub>); IR (KBr): 1586, 1690 (C=O), 2209 (CN), 3310 and 3425 (NH) cm<sup>-1</sup>; <sup>1</sup>H NMR (300 MHz, DMSO-*d*<sub>6</sub>): δ 3.85 (s, 3H, OMe), 4.53 (s, 2H, SCH<sub>2</sub>), 6.56 (s, 1H, CH), 7.10 (m, 4H, Ar-H & NH), 7.44 (d, 2H, *J*=7.5 Hz, Ar-H), 7.80 (m, 1H, Ar-H), 8.02 (d, 2H, *J*=7.5 Hz, Ar-H), 9.52 (bs, 1H, NH); MS: 451.1 (M-H)<sup>+</sup>; Anal. Calcd (C<sub>25</sub>H<sub>16</sub>N<sub>4</sub>O<sub>3</sub>S): C, 66.36; H, 3.56; N, 12.38 Found: C, 66.25; H, 3.51; N, 12.31; HRMS (ESI): calc. for C<sub>25</sub>H<sub>15</sub>N<sub>4</sub>O<sub>3</sub>: 451.0859 (M<sup>+</sup>+H); found: 451.0880.

**7-Imino-6-oxo-10-(4-fluorophenyl)-7,9-dihydro-6*H*,13*H*-pyrazolo[1,5-*a*]thiochromeno[3',4':5,6]pyrano[4,3-*d*]pyridine-12-carbonitrile (8f)**

Yellow solid; yield: 63%; mp: 310°C (start to decompose);  $R_f$  0.11 ( $\text{CHCl}_3$ ); IR (KBr): 1602, 1691 ( $\text{C}=\text{O}$ ), 2207 (CN), 3303 and 3422 (NH)  $\text{cm}^{-1}$ ;  $^1\text{H}$  NMR (300 MHz,  $\text{DMSO-d}_6$ ):  $\delta$  4.30 (s, 2H,  $\text{SCH}_2$ ), 6.50 (s, 1H, CH), 7.10-7.28 (m, 6H, Ar-H & NH), 7.59 (d, 1H,  $J=7.2$  Hz, Ar-H), 7.92 (d, 2H,  $J=5.7$  Hz, Ar-H), 9.38 (bs, 1H, NH); MS: 439.1 ( $\text{M-H}^+$ ); Anal. Calcd ( $\text{C}_{24}\text{H}_{13}\text{N}_4\text{O}_3\text{FS}$ ): C, 65.45; H, 2.97; N, 4.31 Found: C, 65.39; H, 2.94; N, 4.28; HRMS (ESI): calc. for  $\text{C}_{24}\text{H}_{13}\text{N}_4\text{O}_3\text{FS}$ : 441.0816 ( $\text{M}^+\text{+H}$ ); found: 441.0816.

**7-Imino-6-oxo-10-(3-(trifluoromethyl)phenyl)-7,9-dihydro-6H,13H-pyrazolo[1,5-*a*]thiochromeno[3',4':5,6]pyrano[4,3-*d*]pyridine-12-carbonitrile (8g)**

Yellow solid; yield: 76%; mp: 309-310°C;  $R_f$  0.13 ( $\text{CHCl}_3$ ); IR (KBr): 1615, 1692 ( $\text{C}=\text{O}$ ), 2210 (CN), 3305 and 3418 (NH)  $\text{cm}^{-1}$ ;  $^1\text{H}$  NMR (300 MHz,  $\text{DMSO-d}_6$ ): 4.31 (s, 2H,  $\text{SCH}_2$ ), 6.71 (s, 1H, CH), 7.18-7.29 (m, 3H, Ar-H & NH), 7.54-7.62 (m, 3H, Ar-H), 8.16 (s, 1H, Ar-H), 8.19-8.21 (m, 2H, Ar-H), 9.45 (bs, 1H, NH); MS: 489.1 ( $\text{M-H}^+$ ); Anal. Calcd ( $\text{C}_{25}\text{H}_{13}\text{F}_3\text{N}_4\text{O}_2\text{S}$ ): C, 61.22; H, 2.67; N, 11.62 Found: C, 61.12; H, 2.65; N, 11.57; HRMS (ESI): calc. for  $\text{C}_{25}\text{H}_{14}\text{F}_3\text{N}_4\text{O}_2\text{S}$ : 491.0784 ( $\text{M}^+\text{+H}$ ); found: 491.0815.

**7-Imino-6-oxo-10-(3,4,5-trimethoxyphenyl)-7,9-dihydro-6H,13H-pyrazolo[1,5-*a*]thiochromeno[3',4':5,6]pyrano [4,3-*d*]pyridine-12-carbonitrile (8h)**

Yellow solid; yield: 65%; mp: 275°C (start to decompose);  $R_f$  0.84 (Hexane: EtOAc, 1:1); IR (KBr): 1606, 1695 ( $\text{C}=\text{O}$ ), 2202 (CN), 3294 and 3407 (NH)  $\text{cm}^{-1}$ ;  $^1\text{H}$  NMR (300 MHz,  $\text{DMSO-d}_6$ ):  $\delta$  3.74 (s, 9H, 3xOMe), 4.30 (s, 2H,  $\text{SCH}_2$ ), 6.60 (s, 1H, CH), 7.14 (s, 2H, Ar-H), 7.18-7.28 (m, 4H, Ar-H & NH), 7.60 (d, 1H,  $J=4.9$  Hz, Ar-H), 9.38 (bs, 1H, NH); MS: 511.1 ( $\text{M-H}^+$ ); Anal. Calcd ( $\text{C}_{27}\text{H}_{20}\text{N}_4\text{O}_5\text{S}$ ): C, 63.27; H, 3.93; N, 10.93 Found: C, 63.6; H, 3.89; N, 10.88; HRMS (ESI): calc. for  $\text{C}_{27}\text{H}_{21}\text{N}_4\text{O}_5\text{S}$ : 513.1227 ( $\text{M}^+\text{+H}$ ); found: 491.1233.

**2.2. General procedure for the Synthesis of 9-amino-8-oxo-1,2-dihydro-8H-benzo[4,5]imidazo[1,2-a]benzo[7,8]chromeno[4,3-d]pyridine-16-carbonitrile (10a-b) / 9-amino-8-oxo-1H,8H-benzo[4,5]imidazo[1,2-a]thiochromeno[3',4':5,6]pyrano[4,3-d]pyridine-16-carbonitrile (10c-d) [23].**

A mixture of lactone **3** (1.0 mmol), 2-cyanomethyl-1H-benzimidazole (**9**, 1.0 mmol) and powdered KOH (1.2 mmol) in DMF (9 mL) was stirred at room temperature for 5-8 h. The reaction was monitored using silica gel TLC. After consumption of **3**, the residue was poured onto crushed ice with vigorous stirring. The aqueous suspension was neutralized with dil. HCl (if required) and the precipitate obtained was filtered, washed with water and dried. The crude residue was purified by silica gel column chromatography using chloroform/methanol (0-30%);

**9-Amino-8-oxo-1H,8H-benzo[4,5]imidazo[1,2-a]thiochromeno[3',4':5,6]pyrano[4,3-d]pyridine-16-carbonitrile (10a)**

Orange solid; yield: 76%; mp: >315°C (start to decompose);  $R_f$  0.42 (CHCl<sub>3</sub>:MeOH, 10:1); IR (KBr): 1563, 1612, 1692 (C=O), 2208 (CN), 3173 and 3440 (NH) cm<sup>-1</sup>; <sup>1</sup>H NMR (300 MHz, DMSO-d<sub>6</sub>): δ 2.93 (bs, 2H, CH<sub>2</sub>), 3.22 (bs, 2H, CH<sub>2</sub>), 7.11 (m, 1H, Ar-H), 7.32 (m, 4H, Ar-H), 7.49 (m, 1H, Ar-H), 7.64 (m, 1H, Ar-H), 7.89 & 9.93 (bs, 2H, NH<sub>2</sub>), 8.79 (m, 1H, Ar-H); MS: 377.1 (M-H)<sup>+</sup>; Anal. Calcd (C<sub>23</sub>H<sub>14</sub>N<sub>4</sub>O<sub>2</sub>): C, 73.01; H, 3.73; N, 14.81 Found: C, 72.92; H, 3.70; N, 14.73; HRMS (ESI): calc. for C<sub>23</sub>H<sub>15</sub>N<sub>4</sub>O<sub>2</sub>: 379.1189 (M<sup>+</sup>+H); found: 491.1197.

**9-Amino-5-methoxy-8-oxo-1,2-dihydro-8H-benzo[4,5]imidazo[1,2-a]benzo[7,8]chromeno[4,3-d]pyridine-16-carbonitrile (10b)**

Orange solid; yield: 98%; mp: >315°C (start to decompose);  $R_f$  0.40 (CHCl<sub>3</sub>:MeOH, 10:1); IR (KBr): 1612, 1690 (C=O), 2204 (CN), 3181 and 3446 (NH) cm<sup>-1</sup>; <sup>1</sup>H NMR (300 MHz, DMSO-d<sub>6</sub>): δ 2.94 (t, 2H,  $J=6.6$  Hz, CH<sub>2</sub>), 3.26 (t, 2H,  $J=6.6$  Hz, CH<sub>2</sub>), 3.83 (s, 3H, OCH<sub>3</sub>), 6.92 (s, 2H, Ar-H), 7.14 (t, 1H,

$J=7.2$  Hz, Ar-H), 7.28 (t, 1H,  $J=7.2$  Hz, Ar-H), 7.54 (d, 1H,  $J=8.1$  Hz, Ar-H), 7.63 (d, 1H,  $J=9.3$  Hz, Ar-H), 8.82 (d, 1H,  $J=7.8$  Hz, Ar-H), 9.96 (bs, 2H, NH<sub>2</sub>); MS: 407.1 (M-H)<sup>+</sup>; Anal. Calcd (C<sub>24</sub>H<sub>16</sub>N<sub>4</sub>O<sub>3</sub>): C, 70.58; H, 3.95; N, 13.72 Found: C, 70.46; H, 3.92; N, 13.63; HRMS (ESI): calc. for C<sub>24</sub>H<sub>17</sub>N<sub>4</sub>O<sub>3</sub>: 409.1295 (M<sup>+</sup>+H); found: 409.1294.

**9-Amino-8-oxo-1*H*,8*H*-benzo[4,5]imidazo[1,2-*a*]thiochromeno [3',4':5,6]pyrano[4,3-*d*]pyridine-16-carbonitrile (10c)**

Orange solid; yield: 84%; mp: 309°C (start to decompose); R<sub>f</sub> 0.64 (CHCl<sub>3</sub>:MeOH, 10:1); IR (KBr): 1556, 1603, 1691 (C=O), 2208 (CN), 3177 and 3426 (NH) cm<sup>-1</sup>; <sup>1</sup>H NMR (300 MHz, DMSO-*d*<sub>6</sub>): δ 4.48 (s, 2H, SCH<sub>2</sub>), 7.14 (t, 2H,  $J=7.5$  Hz, Ar-H), 7.25-7.41 (m, 5H, Ar-H & NH<sub>2</sub>), 7.55 (d, 1H,  $J=7.8$  Hz, Ar-H), 7.74 (dd, 1H,  $J=1.5$  & 7.5 Hz, Ar-H), 8.80 (d, 1H,  $J=8.1$  Hz, Ar-H); <sup>13</sup>C NMR (75 MHz, DMSO-*d*<sub>6</sub>): δ 25.24, 69.31, 88.97, 107.11, 115.55, 117.50, 117.64, 121.08, 124.37, 126.29, 127.02, 127.90, 128.56, 131.32, 132.86, 135.22, 144.50, 145.41, 151.28, 151.59, 154.97, 161.31; MS: 395.1 (M<sup>+</sup>-1); Anal. Calcd (C<sub>22</sub>H<sub>12</sub>N<sub>4</sub>O<sub>2</sub>S): C, 66.66; H, 3.05; N, 14.13 Found: C, 66.51; H, 3.01; N, 14.03; HRMS (ESI): calc. for C<sub>22</sub>H<sub>13</sub>N<sub>4</sub>O<sub>2</sub>S: 397.0753 (M<sup>+</sup>+H); found: 397.0763.

**9-Amino-5-chloro-8-oxo-1*H*,8*H*-benzo[4,5]imidazo[1,2-*a*]thiochromeno[3',4':5,6]pyrano[4,3-*d*]pyridine-16-carbonitrile (10d)**

Orange solid; yield: 76%; mp: 312°C (start to decompose); R<sub>f</sub> 0.85 (CHCl<sub>3</sub>:MeOH, 10:1); IR (KBr): 1562, 1606, 1694 (C=O), 2217 (CN), 3190 and 34.27 (NH) cm<sup>-1</sup>; <sup>1</sup>H NMR (300 MHz, DMSO-*d*<sub>6</sub>): δ 4.49 (s, 2H, SCH<sub>2</sub>), 7.38-7.43 (m, 5H, Ar-H & NH<sub>2</sub>), 7.58 (d, 1H,  $J=7.8$  Hz, Ar-H), 7.66 (d, 1H,  $J=1.8$  Hz, Ar-H), 8.84 (d, 1H,  $J=8.1$  Hz, Ar-H), 9.95 (bs, 1H, NH<sub>2</sub>); <sup>13</sup>C NMR (75 MHz, DMSO-*d*<sub>6</sub>): δ 25.21, 69.75, 88.94, 107.96, 117.52, 117.68, 120.98, 121.05, 124.31, 125.53, 129.44, 130.08, 130.74, 131.41, 132.88, 134.05, 144.04, 145.44, 149.95, 151.45, 154.88, 160.91; MS: 429.1 (M-H)<sup>+</sup>; HRMS (ESI): calc.

for C<sub>22</sub>H<sub>12</sub>ClN<sub>4</sub>O<sub>2</sub>S: 431.0369 (M<sup>+</sup>+H); found: 431.0394.

### 3. Computational Details

All the calculations have been performed using the Gaussian 09 program package [24]. Geometrical optimization was performed in vacuo using B3LYP [25,26] exchange-correlation functional and a 6-311G(d, p) basis set [26]. The optimized geometries were then used to obtain frontier molecular orbitals (FMOs). To simulate the optical spectra, the lowest spin allowed singlet–singlet transitions were computed on the ground state geometry. TDDFT calculations of the lowest singlet–singlet excitations were performed in DMF solution, on the optimized geometries using the B3LYP/6-311G (d, p) level of theory. The integral equation formalism polarizable continuum model (PCM) [27] within self-consistent reaction field (SCRF) theory, has been used to describe the solvation of the molecules. The software GaussSum 2.2.5 [28] was utilized to simulate the major portion of absorption spectrum and to analyze the nature of transitions.

### 4. Results and discussion

#### 4.1 Chemistry

The proposed pyrazoles (**8a-h**) and imidazoles (**10a-d**) derivatives were synthesized using earlier reported procedures following the reaction of suitably substituted benzo[*h*]chromene (**3a-b**, **4a-b**) and thiochromeno[4,3-*b*]pyrans (**3c-d**, **4c-d**) with active methylene group containing 2-(5-aryl-1*H*-pyrazol-3-yl)acetonitrile (**7**) or 2-imidazolyl acetonitrile (**9**) under basic reaction conditions (Scheme 1 and 2) [23].

The **3a-d** and **4a-d** were selected owing to their interesting chemistry and versatile applicability as a synthon for the synthesis of diverse heterocycles[15]. Structurally, benzo[*h*]chromene (**3a-b**, **4a-b**) and thiochromeno[4,3-*b*]pyrans (**3c-d**, **4c-d**) have three electrophilic centers. Due to the presence of three electrophilic centers, they produce different products when reacted with nucleophiles under different

reaction conditions and in situ yields cyclic arenes and heteroarenes.

<<Insert Figure-2>>

<<Insert Figure-3>>

<<Insert Scheme 1>>

In brief, the starting compounds **3a-b** [29] were prepared from the reaction of 1-tetralone (**2a-b**) with methyl 2-cyano-3,3-dimethylthioacrylate (**1**) and 4-methylthio-2-oxo-2,5-dihydrothiochromeno-[4,3-*b*]pyran-3-carbonitriles (**3c-d**) [30], from the reaction of thiochromen-4-ones (**2c-d**) with methyl 2-cyano-3,3-dimethylthioacrylate (**1**). Subsequent amination of **3a-d** were carried out using piperidine in boiling ethanol, to afford corresponding **4a-d** (Fig. 2). Further, active methylene containing pyrazoles (**7**) were synthesized using hydrazine and 2*H*-pyran-2-ones (**6**) as precursors Fig. 3 [30,31]. Compound **6** was finally synthesized from the reaction of aryl methyl ketone (**5**) with methyl 2-cyano-3,3-dimethylthioacrylate (**1**) [31].

<<Insert Scheme 2>>

Finally the pyrazole (**8a-h**) and benzimidazole (**10a-d**) derivatives were synthesized using an equimolar mixture of lactone (**3** or **4**) and pyrazole (**7**) or imidazole (**9**) by the attack of nucleophile at C4 position of **3** or **4** in KOH/DMF at room temperature (Scheme 1-2) in good yields.

#### 4.2. Optical properties

The photophysical and electrochemical data of compounds such as  $\lambda_{\max}$  of their UV-Vis absorption and photoluminescence (PL) spectra, fluorescence quantum yield, HOMO/LUMO energy levels, and the electrochemical band gap ( $E_g$ ) were investigated. The fluorescence quantum yields in

DMF were determined by the optically dilute method using fluorescein ( $\Phi_{fl} = 0.79$  in ethanol) as a reference.

The UV-Vis absorption spectra of pyrazoles (**8a-h**) and imidazoles (**10a-d**) are recorded in DMF solution as shown in Fig. 4. The various photophysical data of the compounds are shown in Table 1. A broad band between 270 and 350 nm observed in the absorption spectra in DMF was attributed to the  $\pi$ - $\pi^*$  transition. The imidazole moiety (**10a-d**) showed a red shifted absorption peak ( $\lambda_{max}$ , 455-474 nm) and higher molar extinction coefficient compared to that of pyrazole (**8a-c**) moieties resulting from increased  $\pi$ -conjugation. Interestingly, when the sulfur atom was introduced into the chromene unit to construct **8d-h**, the  $\lambda_{max}$  was red-shifted by  $\approx 14$  nm [32]. A similar trend was also observed in the case of imidazole molecules.

The normalized UV-Vis and PL spectra of synthesized molecules are shown in Fig. 5. The emission properties are summarized in Table 1. The PL maxima of pyrazoles (**8a-h**) showed strong green fluorescence at 493-511 nm with a moderate to good fluorescence quantum yield up to 78% [33]. In the case of increasing  $\pi$ -conjugation from pyrazoles to imidazoles (**10a-d**) red shift in the emission maxima (537 nm-565 nm) was observed. The emission peak was not strongly affected by the hetero atom (s) in the pyrazole moieties ( $\approx 495$  nm for **8a** & **8b** and  $\approx 508$  nm for **8d-h**).

<<Insert Table 1>>

<<Insert Figure-4>>

Interestingly, compounds **10c** and **10d** showed PL maxima in the red region (562 nm, 565 nm respectively). The imidazoles (**10a-d**), exhibited relatively large Stokes shifts (80-91 nm) compared to pyrazoles (53-70 nm) possibly due to high intramolecular charge-transfer excitation of an electron from HOMO level to the LUMO level of the molecules.

In order to provide in-depth insight into the electronic structures, we have chosen one molecule from each category (**8a**, **8d**, **10a** and **10c**) for further theoretical study. We have carried out TDDFT (Time Dependent Density Functional Theory) studies in DMF using B3LYP/6-311G(d,p) level of theory. Structures of optimized geometries of these molecules at B3LYP/6-311 G(d,p) level theory were shown in Fig 6. The TDDFT calculations with B3LYP are in nearly good agreement with experimental UV-Vis spectra. The spectra have been produced by convoluting Gaussian functions with full width at half maximum (FWHM) = 0.03 eV. The normalized plots of simulated and experimental UV-Vis spectra of these molecules are shown in Fig. 7. The wavelengths of the excitations with the largest oscillator strengths ( $f$ ) within these bands are given in Table 2. Based on TDDFT calculations, the intense singlet transition at around 407 nm (**8a**,  $f = 0.334$ ), 418 nm (**8d**,  $f = 0.453$ ), 467 nm (**10c**,  $f = 0.383$ ) respectively is attributed to the HOMO to LUMO transition, whereas for the **10a** at around 400 nm ( $f=0.606$ ) attributed to transition from HOMO to LUMO+2 (Table 2) The optimized geometry parameters, at the B3LYP/6-311 G(d,p) level of theory are shown in Table 3.

<<Insert Figure-5>>

<<Insert Table 2>>

#### 4.3. Electrochemical Properties

Electrochemical studies using cyclic voltammetry (CV) were performed to evaluate the redox behavior of the pyrazoles (**8a-h**) and imidazoles (**10a-d**). All measurements were performed in a three-electrode cell setup using Ag/AgCl as reference electrode and a Pt electrode as the working electrode, using a 0.1 M of the electrolyte tetrabutylammoniumhexafluorophosphate ( $\text{Bu}_4\text{NPF}_6$ ) dissolved in DMF. The DPV voltammograms obtained were employed to evaluate the highest occupied molecular orbital (HOMO) and the lowest unoccupied molecular orbital (LUMO) energy levels [34]. As shown in Fig. 8, the first oxidation potential ( $E_{\text{ox}}$ ) corresponds to the HOMO level of the molecule. The HOMO level was readily

estimated using the equation  $E_{\text{HOMO}} = -(E_{\text{ox}} + 4.8)$  eV. The LUMO could be calculated from the equation  $E_{\text{ox}} - E_{0-0}$  where  $E_{0-0}$  is the zeroth-zeroth transition value obtained from the intersection of the normalized absorption and emission spectra as shown in Fig. 5 and tabulated in Table 1. The  $E_{\text{ox}}$  of these compounds were calculated relative to the ferrocene/ferrocenium ( $\text{Fc}/\text{Fc}^+$ ) 0.53 V vs Ag/AgCl electrode [35]. The HOMO and LUMO levels of the new molecules were found to be in the range of -5.64 eV to -5.43 eV and -2.61 eV to -2.95 eV, respectively. The imidiazoles exhibited higher HOMO level compared to pyrazoles, attributed from increase in the  $\pi$ -conjugation.

We have plotted the isosurfaces (isovalue=0.02) of the HOMO and LUMO Fig. 10 as well as the nearest frontier orbitals of **8a**, **8d**, **10a** and **10c** which are involved in transitions with strong contributions to the first excitation as well as to next two excitations with strong oscillator strength. The HOMO and LUMO energies of the pyrazole molecules (**8a**, **8d**) located over the chromene and pyrazole moiety, whereas for imidazole moieties (**10a**, **10c**) the HOMO is distributed over the total molecule. There is no clear trend in the LUMO energies of the imidazole molecules.

The calculated HOMO, LUMO energies and the HOMO-LUMO gap (HLG) at a B3LYP/6-311g (d,p) level in DMF solvent is given in Fig. 9. The computationally and experimentally determined HOMO, LUMO energies are in good agreement. The HOMO-LUMO gaps are shown in Table 2.

<<Insert Table 3>>

<<Insert Figure-6>>

<<Insert Figure-7>>

<<Insert Figure-8>>

<<Insert Figure-9>>

<<Insert Figure-10>>

### 3. Conclusions:

In summary, we have synthesized and successfully measured the photophysical and electrochemical properties of highly congested pyrazole and imidazole ring containing heterocycles. The UV-Vis spectra of these molecules showed that the imidazole bearing molecules exhibited red shift in the absorption band higher molar extinction coefficient compared to pyrazole containing molecules. This work demonstrates that these molecules having strong, broad absorption and appropriate energy levels, could, with further development, be employed as materials for organic electronics as well as sensitizers.

### Notes

The authors declare no competing financial interest.

### Acknowledgements

AG and HKM acknowledge SERB, DST New Delhi, India for financial support as DST Fast Track Young Scientist Fellowship. Ch. P.K. thanks UGC, New Delhi for a senior research fellowship. Authors are thankful to Director CSIR-CIMAP, CSIR-CDRI, Lucknow and CSIR-IICT, Hyderabad.

### References and notes

- [1] Zhu XH, Peng J, Cao Y, Roncali J. Solution-processable single-material molecular emitters for organic light-emitting devices. *Chem Soc Rev* 2011; 40: 3509-24.
- [2] Zhu M, Yang C. Blue fluorescent emitters: design tactics and applications in organic light-emitting diodes. *Chem Soc Rev* 2013; 42: 4963-76.
- [3] Reineke S, Thomschke M, Lüssem B, Leo K. White organic light-emitting diodes: Status and perspective. *Rev Mod Phys* 2013; 85:1245–93.A
- [4] Huang X, Han S, Huang W, Liu X. Enhancing solar cell efficiency: the search for luminescent materials as spectral converters. *Chem Soc Rev* 2013; 42: 173-201.

- [5] Goetzberger A, Wittwer V. Fluorescent planar collector-concentrators: A review. *Solar Cells* 1981; 4: 3-23.C
- [6] Christie RM. Fluorescent dyes. *Review of Progress in Coloration and Related Topics* 1993; 23: 1-18.
- [7] Nhan DT, Hien NK, Duc HV, Nhung NTA, Trung NT, Van DU, Shin WS, Kim JS, Quang DT. A hemicyanine complex for the detection of thiol biomolecules by fluorescence. *Dyes Pigm* 2016;131:301-6.T
- [8] Balanda AO, Volkova KD, Kovalska VB, Losytskyy MY, Tokar VP, Prokopets VM, Yarmoluk SM. Synthesis and spectral–luminescent studies of novel 4-oxo-4,6,7,8-tetrahydropyrrolo[1,2-a]thieno[2,3-d]pyrimidinium styryls as fluorescent dyes for biomolecules detection. *Dyes Pigm* 2007; 75: 25-31.
- [9] Chinen AB, Guan CM, Ferrer JR, Barnaby SN, Merkel TJ, Mirkin CA. Nanoparticle Probes for the Detection of Cancer Biomarkers, Cells, and Tissues by Fluorescence *Chem Rev* 2015; 115: 10530-74.
- [10] Watanabe H, Ono M, Sajia H. In vivo fluorescence imaging of  $\beta$ -amyloid plaques with push–pull dimethylaminothiophene derivatives. *Chem Commun* 2015; 51: 17124-7.
- [11] Terai T, Nagano T. Fluorescent probes for bioimaging applications. *Curr Opin Chem Biol* 2008;12:515-21.
- [12] Gonçalves MST. Fluorescent labeling of biomolecules with organic probes. *Chem Rev* 2009;109:190-212.
- [13] Martínez-Máñez R, Sancenón F. Fluorogenic and chromogenic chemosensors and reagents for anions. *Chem Rev* 2003;103:4419-76.
- [14] Liu Z, Qi W, Xu G. Recent advances in electrochemi luminescence. *Chem Soc Rev* 2015;44:3117-42.
- [15] Wang Y, Tang B, Zhang S. Light–thermal conversion organic shape-stabilized phase-change materials with broadband harvesting for visible light of solar radiation. *RSC Adv* 2012;2:11372-78.

- [16] Chou Y-H, Tsai C-L, Chen W-C, Liou G-S. Nonvolatile transistor memory devices based on high- $k$  electrets of polyimide/TiO<sub>2</sub> hybrids. *Polym Chem* 2014; 5:6718-27.
- [17] Jiang J-Q, Sun C-L, Shi Z-F, Zhang H-L. Squaraines as light-capturing materials in photovoltaic cells. *RSC Adv* 2014;4:32987-96.
- [18] Tao Y, Yang C, Qin J. Organic host materials for phosphorescent organic light-emitting diodes. *Chem Soc Rev* 2011;40:2943-70.
- [19] Coppeta R, Rogers C. Dual emission laser induced fluorescence for direct planar scalar behavior measurements. *Exp Fluids* 1998; 25:1-15.
- [20] Gawley RE, Mao H, Haque MM, Thorne JB, Pharr JS. Visible Fluorescence Chemosensor for Saxitoxin. *J Org Chem*, 2007; 72:2187-91.
- [21] Shi W, Fan S, Huang F, Yang W, Liu R, Cao Y. Synthesis of novel triphenylamine-based conjugated polyelectrolytes and their application as hole-transport layers in polymeric light-emitting diodes. *J Mater Chem*, 2006; 16:2387-94.
- [22] Cölle M, Dinnebir RE, Brütting W. The structure of the blue luminescent  $\delta$ -phase of tris(8-hydroxyquinoline)aluminium(III)(Alq<sub>3</sub>). *Chem Comm* 2002; 2908-9.
- [23] Maurya HK, Gupta A. A carbanion induced synthesis of highly congested pyrazole and imidazole containing heterocycles. *Tetrahedron Lett*, 2014; 55:1715-19.
- [24] Frisch MJ, Trucks GW, Schlegel HB, Scuseria GE, Robb MA, Cheeseman JR, Scalmani G, Barone V, Mennucci B, Petersson GA, Gaussian 09, Revision B.01, Gaussian, Inc., Wallingford, CT, 2010.
- [25] (a) Becke AD. Density-functional thermochemistry. III. The role of exact exchange. *J Chem Phys*, 1993;98:5648; (b) Becke AD. Density-functional thermochemistry. IV. A new dynamical correlation functional and implications for exact-exchange mixing. *J Chem Phys*, 1996;104:1040.

- [26] Petersson GA, Bennett A, Tensfeldt TG, Al-Laham MA, Shirley WA, Mantzaris J. A complete basis set model chemistry. I. The total energies of closed-shell atoms and hydrides of the first-row elements. *J Chem Phys*, 1988;89:2193.
- [27] Cossi M, Barone V, Cammi R, Tomasi J. Ab initio study of solvated molecules: a new implementation of the polarizable continuum model. *Chem Phys Lett*, 1996;255:327-35.
- [28] O'Boyle NM, Tenderholt AL, Langner KM. A library for package-independent computational chemistry algorithms. *J Comput Chem*, 2008;29:839-45.
- [29] Pratap R, Ram VJ. Natural and synthetic chromenes, fused chromenes, and versatility of dihydrobenzo[*h*]chromenes in organic synthesis. *Chem Rev*, 2014; 114:10476-526
- [30] Pratap R, Ram VJ. An efficient and versatile route to the synthesis of 9,10-dihydro-3-formylphenanthrenes. *Tetrahedron Lett*, 2007,48:1715-19.
- [31] Maurya HK, Vasudev PG, Gupta A. A regio selective synthesis of 2,6-diarylpyridine. *RSC Adv*, 2013;3:12955-62.
- [32] Chandrasekharam M, Reddy MA, Singh SP, Priyanka B, Bhanuprakash K, Kantam ML, Islam A, Han L. One bipyridine and triple advantages: tailoring ancillary ligands in ruthenium complexes for efficient sensitization in dye solar cells. *J Mater Chem*, 2012; 22:18757-60.
- [33] Kellogg RE, Bennett RG. Radiation less intermolecular energy transfer ii. triplet→singlet transfer. *J Chem Phys*, 1964;41:3042-45.
- [34] (a) Wan Z, Jia C, Duan Y, Zhou L, Lin Y, Shi Y. Phenothiazine–triphenylamine based organic dyes containing various conjugated linkers for efficient dye-sensitized solar cells. *J Mater Chem*, 2012; 22:25140-47; (b) Li G, Zhou Y-F, Cao X-B, Bao P, Jiang K-J, Lin Y, Yang L-M. Novel TPD-based organic D– $\pi$ –A dyes for dye-sensitized solar cells. *Chem Comm*, 2009; 2201-03.

- [35] Initially, before measuring redox potential of synthesized compounds, reference electrode Ag/AgCl was calibrated in DMF using a ferrocene/ferrocenium ( $\text{Fc}/\text{Fc}^+$ ) redox couple as an external standard.

**Legend for figures**

**Fig. 1.** Some notable organic dyes applied for different purposes.

**Fig. 2.** Synthesis of the substituted 5,6-dihydro-2-oxo-2*H*-benzo[*h*] chromene-3-carbonitriles (**3a-b,4a-b**) and 2,5-dihydro-2-oxo-thiochromeno[4,3-*b*]pyran-3-carbonitriles (**3c-d,4c-d**).

**Fig. 3.** Synthesis of pyran-2-one (**3**) and 2-(5-aryl-1*H*-pyrazol-3-yl) acetonitrile (**4**).

**Fig. 4.** UV-vis spectra of **8a-h** and **10a-d** in DMF.

**Fig 5.** Electronic absorption & emission spectra of **8a-h** and **10a-d** in DMF.

**Fig. 6:** Structures of optimized geometries of **8a, 8d, 10a** and **10c** at B3LYP/6-311 G(d,p) level theory

**Fig 7.** Comparison between experimental (black lines) and calculated (red lines) UV-Vis absorption spectra of the **8a, 8d, 10a** and **10c** molecules in DMF solution. Red vertical lines represent the calculated singlet excitation energies in GaussSum 2.2.5.

**Fig. 8.** Cyclic voltammograms of **8a, 8d, 10a** and **10c** in DMF; scan rate 100 mV s<sup>-1</sup>; supporting electrolyte: tetrabutylammonium hexafluorophosphate (NBu<sub>4</sub>PF<sub>6</sub>).

**Fig. 9.** Calculated HOMO–LUMO gaps at B3LYP/6-311G(d, p) level of theory and respective HOMO and LUMO orbital pictures at B3LYP/6-311G(d, p)level of **8a, 8d, 10a** and **10c** in DMF solvent.

**Fig. 10.** Molecular orbitals of **8a, 8d, 10a** and **10c** in B3LYP functional, involved in transitions that contribute to the first excitation and to the next high absorbance excitation

**Ligend for Tables**

**Table 1.** Photophysical properties of compounds **8a-h** and **10a-d** in DMF

**Table 2.** Calculated properties of the **8a**, **8d**, **10a** and **10c** using B3LYP/6-311G (d,p). Specifically HOMO and LUMO energies (eV), HOMO–LUMO gap (eV), HLG, with corresponding oscillator strengths,  $f$ , the wavelengths of the first excitation and excitations with the largest oscillator strengths and the dipole moment (D),  $\mu$ .

**Table 3.** Optimized geometry parameters of **8a**, **8d**, **10a** and **10c** calculated at B3LYP/6-311G(d,p) level theory.

**Ligend for Shemes**

**Scheme 1.** Synthesis of 7-imino-6-oxo-10-aryl-7,9,13,14-tetrahydro-6*H*-benzo[7,8]chromeno[4,3-*d*]pyrazolo[1,5-*a*]pyridine-12-carbonitrile (**8a-c**)/ 7-imino-6-oxo-10-aryl-7,9-dihydro-6*H*,13*H*-pyrazolo[1,5-*a*]thiochromeno[3',4':5,6]pyrano[4,3-*d*]pyridine-12-carbonitrile (**8d-h**).

**Scheme 2.** Synthesis of 9-amino-8-oxo-1,2-dihydro-8*H*-benzo[4,5]imidazo[1,2-*a*]benzo[7,8]chromeno[4,3-*d*]pyridine-16-carbonitrile (**10a-b**) / 9-amino-8-oxo-1*H*,8*H*-benzo[4,5]imidazo[1,2-*a*]thiochromeno[3',4':5,6]pyrano[4,3-*d*]pyridine-16-carbonitrile (**10c-d**).



Figure 3

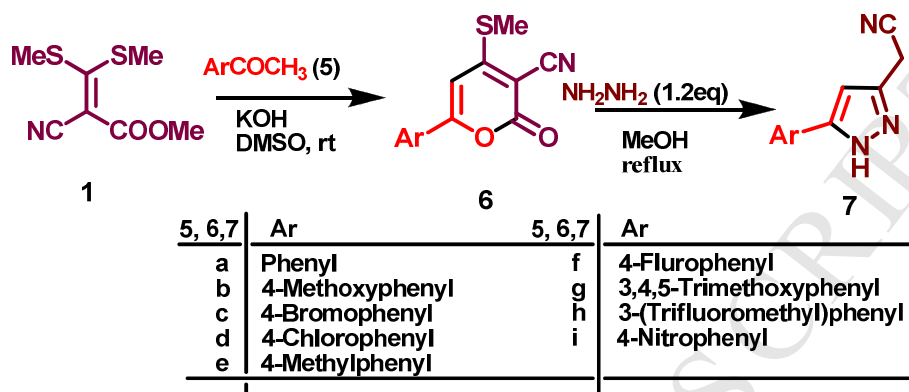


Figure 4

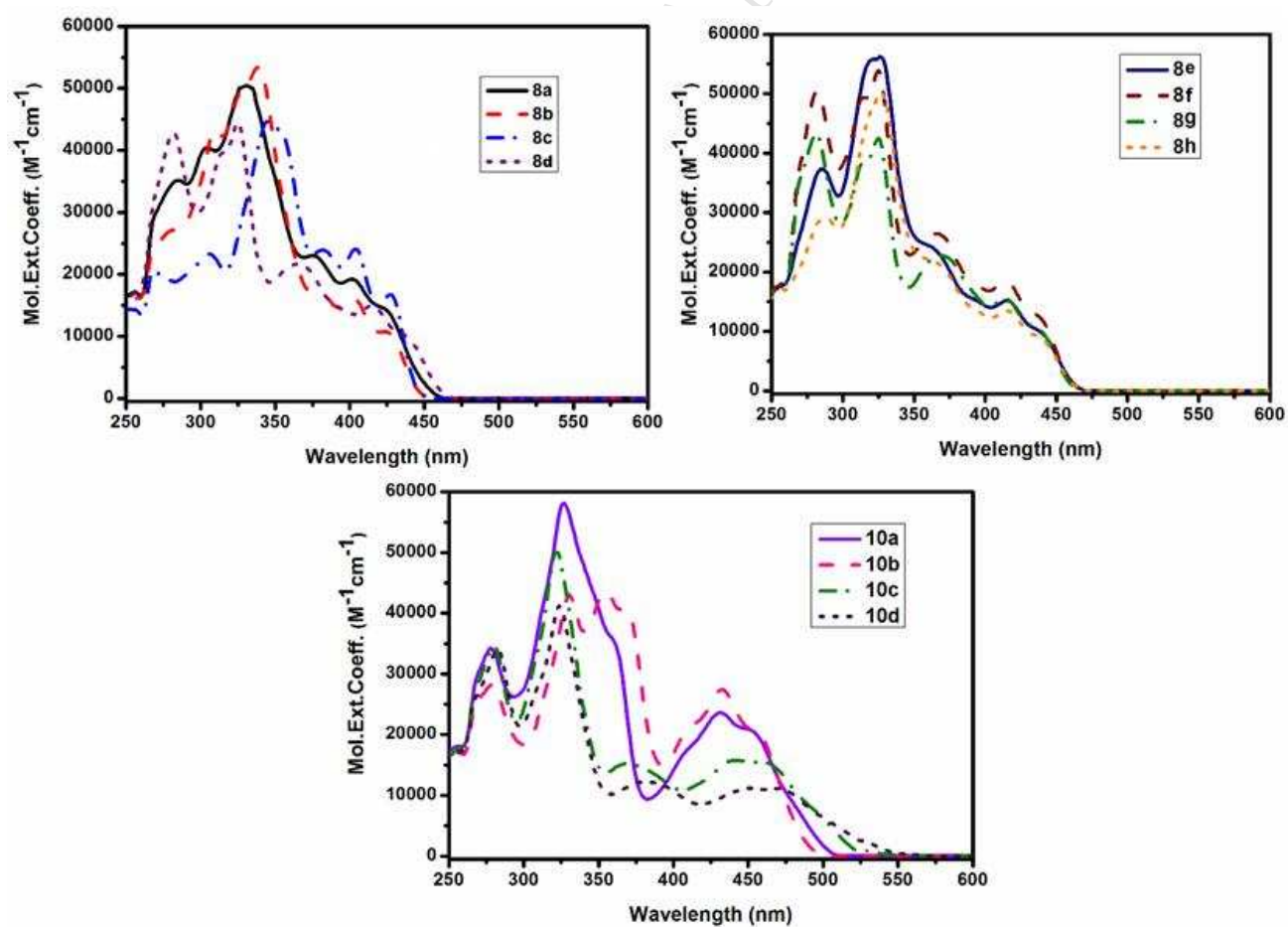


Figure 5

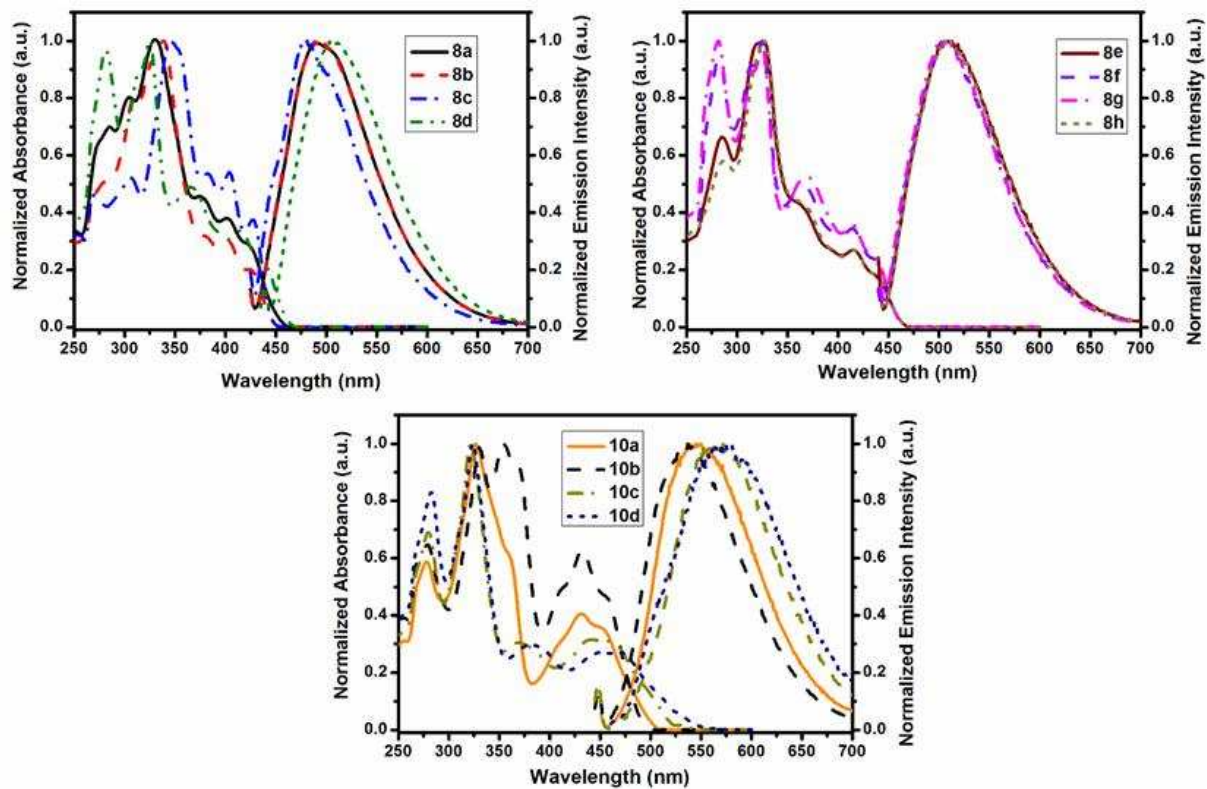


Figure 6

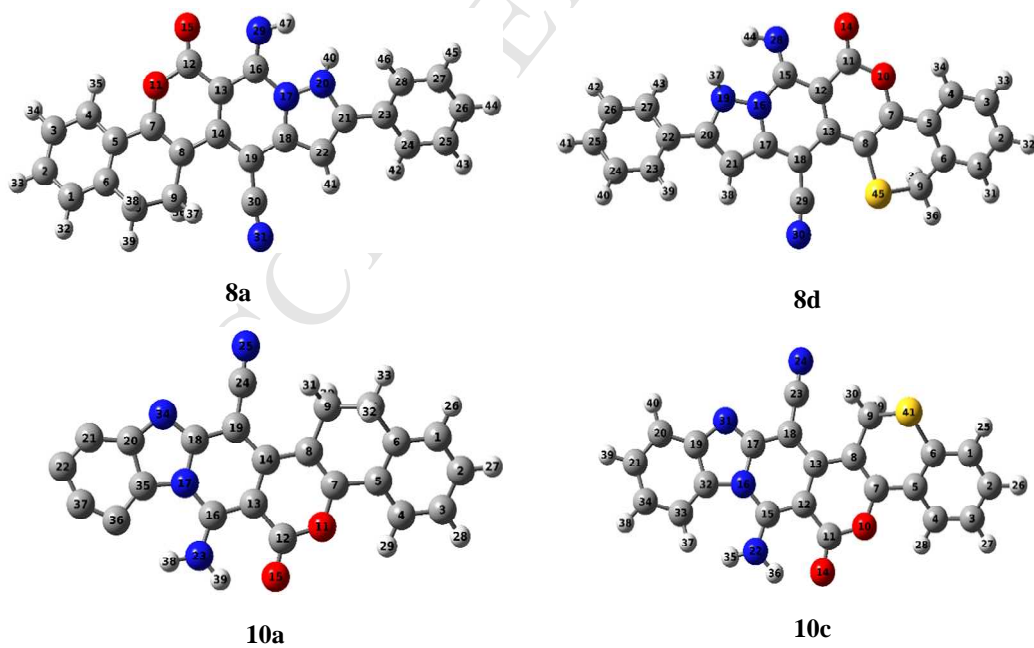


Figure 7

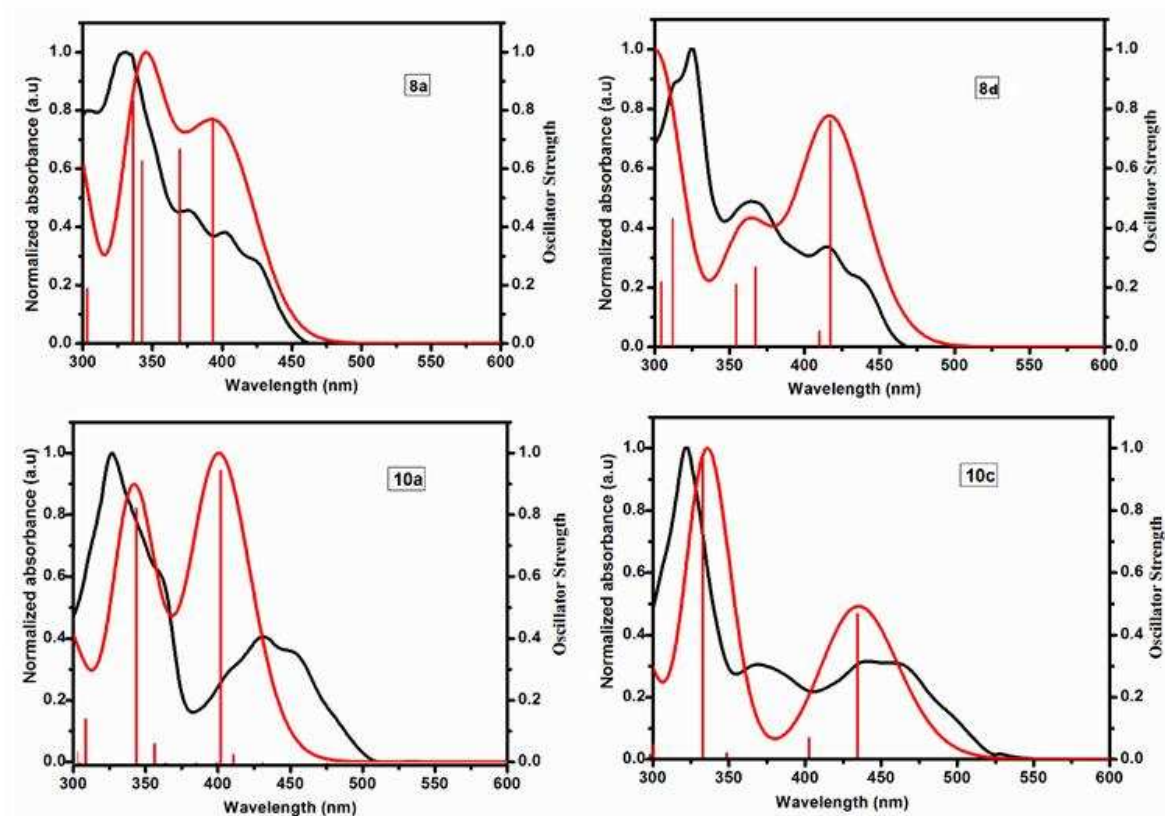


Figure 8

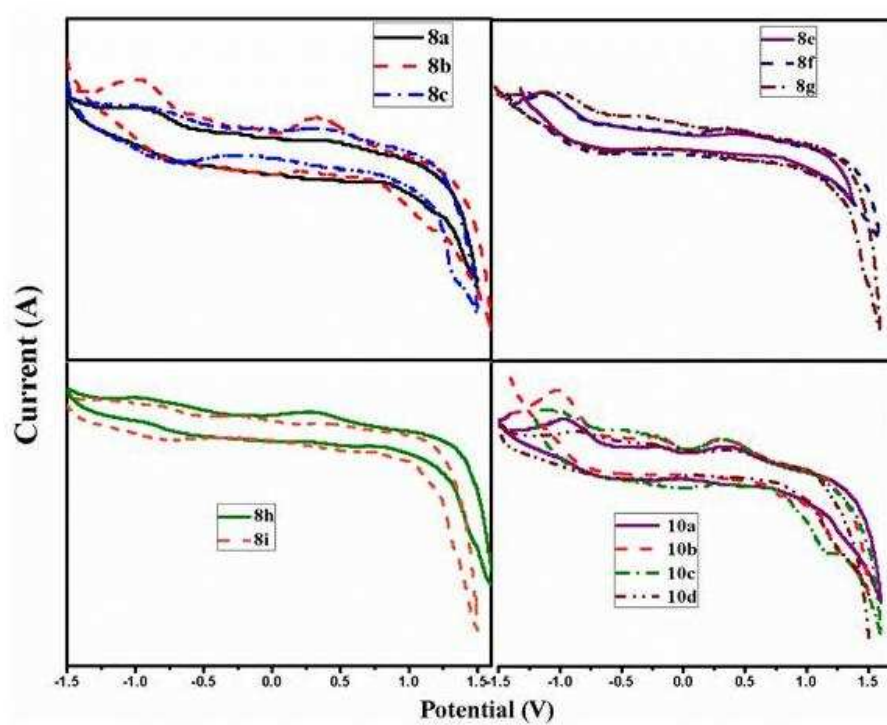


Figure 9

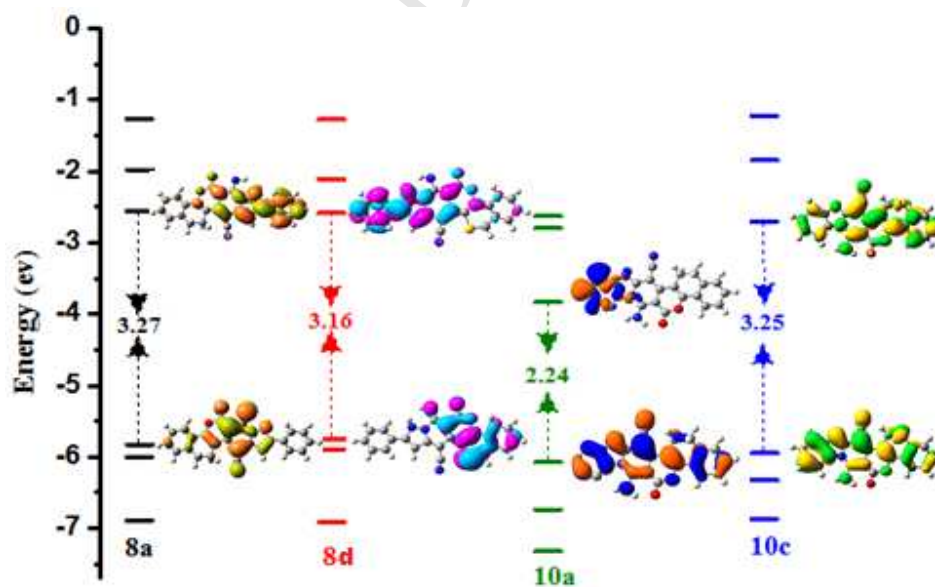
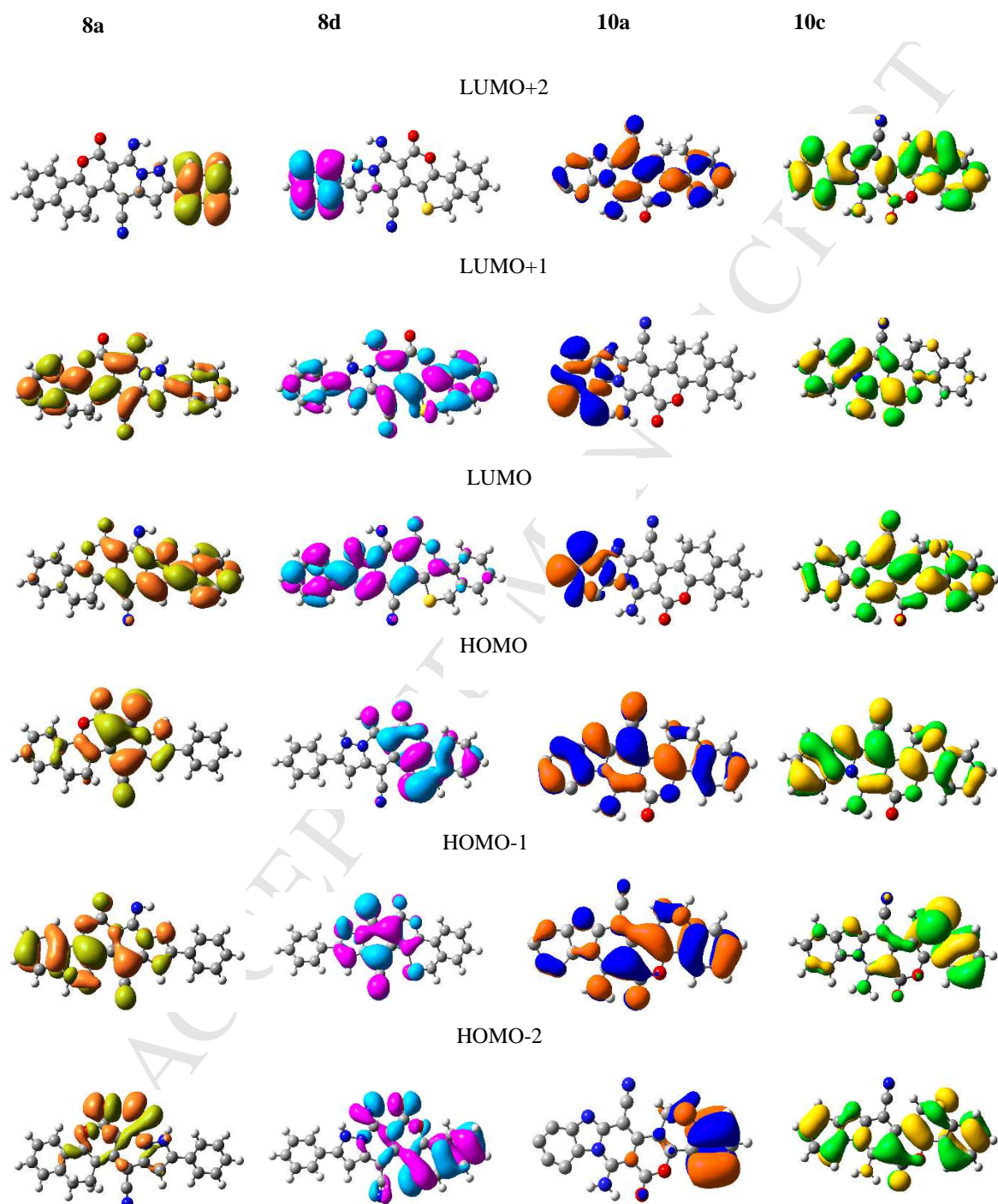


Figure 10



**Table 1**

Compound	<sup>a</sup> $\lambda_{\text{abs}}$ (nm)	<sup>b</sup> $\lambda_{\text{em}}$ (nm)	<sup>c</sup> $\epsilon$ ( $M^{-1}cm^{-1}$ )	<sup>d</sup> $E_{\text{ox}}$	<sup>e</sup> HOMO	<sup>f</sup> LUMO	<sup>g</sup> $E_{0-0}$	<sup>h</sup> $\Delta\nu$ (nm)	<sup>i</sup> $\Phi$
<b>8a</b>	428	493	13,000	0.64	-5.44	-2.61	2.83	65	0.55
<b>8b</b>	428	495	10,470	0.68	-5.48	-2.63	2.85	67	0.66
<b>8c</b>	428	507	17,003	0.76	-5.56	-2.71	2.85	53	0.78
<b>8d</b>	442	508	9,792	0.72	-5.52	-2.77	2.75	66	0.34
<b>8e</b>	444	508	10,591	0.76	-5.56	-2.81	2.75	64	0.41
<b>8f</b>	441	511	12,133	0.84	-5.64	-2.88	2.76	70	0.38
<b>8g</b>	441	508	10,227	0.64	-5.44	-2.68	2.76	67	0.29
<b>8h</b>	444	508	8,927	0.60	-5.40	-2.64	2.76	64	0.22
<b>10a</b>	455	545	20,833	0.73	-5.53	-2.95	2.58	90	0.17
<b>10b</b>	457	537	20,781	0.70	-5.50	-2.89	2.61	80	0.32
<b>10c</b>	467	562	15,790	0.63	-5.43	-2.90	2.53	98	0.05
<b>10d</b>	474	565	11,249	0.64	-5.44	-2.90	2.54	91	0.03

<sup>a</sup> $\lambda_{\text{abs}}$  (nm): Absorption wavelength, <sup>b</sup> $\lambda_{\text{em}}$  (nm): Emission wavelength, <sup>c</sup> $\epsilon$ : Molar extinction coefficient, <sup>d</sup> $E_{\text{ox}}$ : The formal oxidation potentials in DMF were internally calibrated with ferrocene (0.53 V vs Ag/AgCl), <sup>e</sup>HOMO =  $-(E_{\text{ox}}+4.8)\text{eV}$ , <sup>f</sup>LUMO = Calculated with the expression of LUMO = HOMO -  $E_{0-0}$ , <sup>g</sup> $E_{0-0}$ : Band gap, was derived from the intersection between the absorption and emission spectra <sup>h</sup> $\Delta\nu$ : Stokes shifts, <sup>i</sup> $\Phi$ : fluorescence quantum yield.

**Table 2**

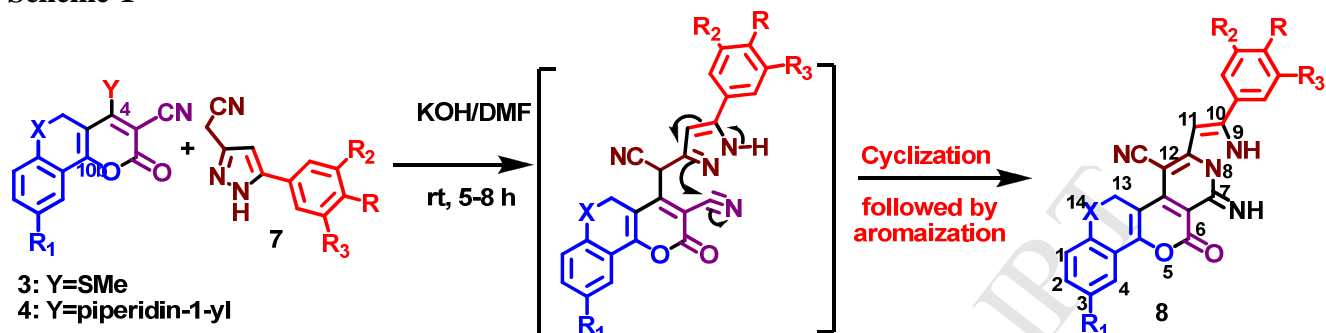
Compound	$\lambda_{\text{max}}^{\text{a}}$ (nm)	$\lambda_{\text{max}}$ (nm)	HOMO	LUMO	HLG	$F$	Main Contribution	$\mu$ (D)
<b>8a</b>	428	407	-5.83	-2.56	3.27	0.334	H $\rightarrow$ L (98%)	6.95
<b>8d</b>	442	418	-5.75	-2.59	3.16	0.453	H $\rightarrow$ L (96%)	5.96
<b>10a</b>	455	400	-6.07	-3.83	2.24	0.606	H $\rightarrow$ L+2 (94%)	3.58
<b>10c</b>	467	437	-5.95	-2.70	3.25	0.383	H $\rightarrow$ L (89%)	5.54

<sup>a</sup>absorption values obtained from experimental data.

**Table 3**

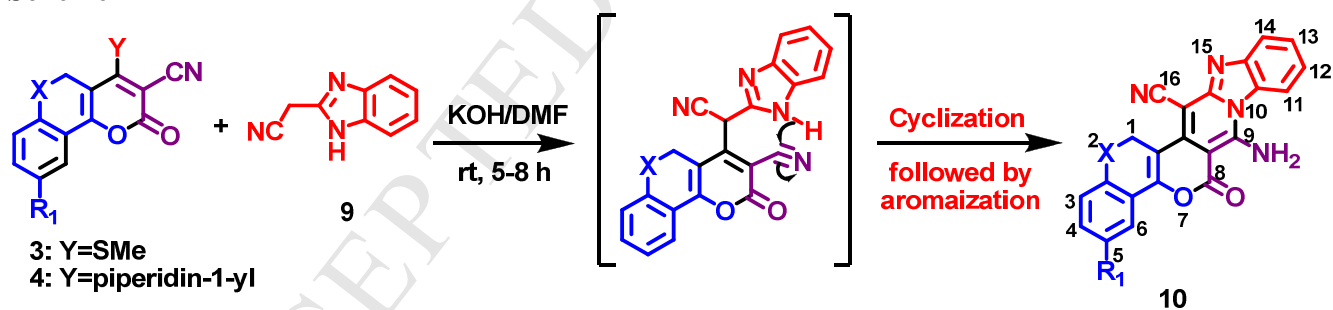
<b>8a</b>		<b>8d</b>		<b>10a</b>		<b>10c</b>	
Bond lengths ( $\text{\AA}$ )							
C <sub>16</sub> -N <sub>29</sub>	1.27	O <sub>10</sub> -C <sub>11</sub>	1.41	O <sub>11</sub> -C <sub>12</sub>	1.37	C <sub>9</sub> -S <sub>41</sub>	1.82
N <sub>17</sub> -N <sub>20</sub>	1.38	C <sub>10</sub> -O <sub>14</sub>	1.19	C <sub>12</sub> -O <sub>15</sub>	1.21	C <sub>7</sub> -O <sub>10</sub>	1.36
C <sub>30</sub> -N <sub>31</sub>	1.15	C <sub>15</sub> -N <sub>28</sub>	1.27	C <sub>24</sub> -N <sub>25</sub>	1.15	C <sub>11</sub> -O <sub>14</sub>	1.21
C <sub>21</sub> -C <sub>23</sub>	1.46	N <sub>16</sub> -N <sub>19</sub>	1.39	C <sub>16</sub> -N <sub>23</sub>	1.32	C <sub>23</sub> -N <sub>24</sub>	1.15
Dihedral angles ( $^{\circ}$ )							
N <sub>29</sub> -C <sub>16</sub> -N <sub>17</sub> -N <sub>20</sub>	-1.45	N <sub>28</sub> -C <sub>15</sub> -C <sub>12</sub> -C <sub>11</sub>	12.27	C <sub>7</sub> -O <sub>11</sub> -C <sub>12</sub> -O <sub>15</sub>	-176.18	O <sub>14</sub> -C <sub>11</sub> -O <sub>10</sub> -C <sub>7</sub>	-176.41
O <sub>15</sub> -C <sub>12</sub> -C <sub>13</sub> -C <sub>16</sub>	4.11	O <sub>14</sub> -C <sub>11</sub> -O <sub>10</sub> -C <sub>7</sub>	177.56	O <sub>11</sub> -C <sub>7</sub> -C <sub>5</sub> -C <sub>4</sub>	15.16	O <sub>14</sub> -C <sub>11</sub> -C <sub>12</sub> -C <sub>15</sub>	-0.58
C <sub>18</sub> -N <sub>17</sub> -N <sub>20</sub> -C <sub>21</sub>	5.78	N <sub>28</sub> -C <sub>15</sub> -N <sub>16</sub> -N <sub>19</sub>	-1.409	O <sub>15</sub> -C <sub>12</sub> -C <sub>13</sub> -C <sub>16</sub>	-1.58	C <sub>8</sub> -C <sub>9</sub> -S <sub>41</sub> -C <sub>6</sub>	51.70
N <sub>31</sub> -C <sub>30</sub> -C <sub>19</sub> -C <sub>18</sub>	-4.70	C <sub>7</sub> -C <sub>8</sub> -S <sub>45</sub> -C <sub>9</sub>	-31.19	N <sub>23</sub> -C <sub>16</sub> -N <sub>17</sub> -C <sub>35</sub>	-0.15	N <sub>22</sub> -C <sub>15</sub> -N <sub>16</sub> -C <sub>32</sub>	2.05
N <sub>20</sub> -C <sub>21</sub> -C <sub>23</sub> -C <sub>28</sub>	25.17	N <sub>19</sub> -C <sub>20</sub> -C <sub>22</sub> -C <sub>27</sub>	-25.33	N <sub>34</sub> -C <sub>18</sub> -C <sub>19</sub> -C <sub>24</sub>	-3.27	C <sub>19</sub> -N <sub>31</sub> -C <sub>17</sub> -C <sub>18</sub>	-177.24
O <sub>15</sub> -C <sub>12</sub> -O <sub>11</sub> -C <sub>7</sub>	-178.05	O <sub>10</sub> -C <sub>7</sub> -C <sub>5</sub> -C <sub>4</sub>	22.30	S <sub>25</sub> -C <sub>24</sub> -C <sub>19</sub> -C <sub>18</sub>	-19.05	N <sub>24</sub> -C <sub>23</sub> -C <sub>18</sub> -C <sub>17</sub>	-35.79
C <sub>22</sub> -C <sub>21</sub> -C <sub>23</sub> -C <sub>24</sub>	26.59	C <sub>17</sub> -N <sub>16</sub> -C <sub>15</sub> -N <sub>28</sub>	168.14	C <sub>19</sub> -C <sub>14</sub> -C <sub>8</sub> -C <sub>9</sub>	4.45	N <sub>31</sub> -C <sub>17</sub> -C <sub>18</sub> -C <sub>23</sub>	-4.03

Scheme-1



Entry	R	R <sub>2</sub>	R <sub>3</sub>	R <sub>1</sub>	X
8a	H	H	H	H	CH <sub>2</sub>
8b	OMe	H	H	H	CH <sub>2</sub>
8c	H	H	H	OMe	CH <sub>2</sub>
8d	H	H	H	H	S
8e	OMe	H	H	H	S
8f	F	H	H	H	S
8g	H	CF <sub>3</sub>	H	H	S
8h	OMe	OMe	OMe	H	S

Scheme-2



Entry	R <sub>1</sub>	X
10a	H	CH <sub>2</sub>
10b	OMe	CH <sub>2</sub>
10c	H	S
10d	Cl	S

### Highlights

1. Highly congested pyrazole and imidazole ring containing heterocycles were synthesized.
2.  $\lambda_{\text{max}}$  of UV-Vis absorption and photoluminescence (PL) spectra, fluorescence quantum yields of these compounds were studied.
3. HOMO/LUMO energy levels and the electrochemical band gap (Eg) were investigated.